Gamma-Ray Emission from Radioactive Isobars

Abstract:

Using a HPGe detector to analyze the gamma-ray spectra of five different radioactive isobars (Co-57, Mn-54, Na-22, Cs-137, and Co-60) the decay schemes for each radioactive source could be determined in this experiment. By knowing the nuclear charge change, or change in atomic number (Z), as well as viewing the gamma-ray spectra for x-rays and specific energy values of gamma-rays, each decay scheme could be recognized. It was established that both Mn-54 and Co-57 decayed to their daughter nuclides by means of electron capture (Scheme 3). After the electron capture stage, Mn-54's daughter nuclide released a gamma-ray of 837.400±0.005 keV and Co-57's daughter nuclide released a gamma-ray of 126.200±0.001 keV to get to their ground states. Na-22 decayed by means of positron emission (Scheme 2), based on the fact that the gamma-ray spectra showed a known energy of 514.000 ±0.004 keV due to positron annihilation. Cs-137 was different than the others because it had two options of decay schemes. Since it produced x-rays, as well as had known values of gamma-rays, Cs-137 could decay by two forms of beta decay. This means that after it emitted a beta particle, its excited daughter nuclide could return to the ground state by either an emission of a gamma-ray of 664.2000±0.0008 keV (Scheme 1a) or by internal conversion, followed by an x-ray (Scheme 1b). Co-60 decayed by beta decay with subsequent gamma ray emission (Scheme 1a). This was accomplished by emitting a beta particle then for the daughter nuclide to return to its ground state, it released two gamma-rays of values 1173.800±0.003 keV and 1333.100±0.004 keV.

Introduction:

This experiment takes advantage of certain radioactive isobars that emit gamma-rays, as well as beta particles in order to determine the decay schemes from the parent nuclide to the daughter nuclide. Isobars are atomic species that have the same mass number, but different atomic number. It was important to realize that all of the decays in this experiment, the mass number does not change, only the atomic number.

The motivation behind studying the decays of radioactive sources is seen mainly in the health industry. By understanding which atoms decay into other atoms, as well as knowing how they decay, can be very useful in the medical community. Certain radioactive isotopes are put into pill or dye form and are used in diagnostic medicine. For certain MRIs or PET scans the patient must be injected with a special solution that contains a radioactive isotope that will allow higher contrast in the image. These sources can also be used to treat cancer. Cobalt-60 is a radioactive source studied in this experiment and it is widely used in the treatment of cancer. The gamma-rays Co-60 puts off is targeted on a cancerous cell [4]. The gamma-rays damage the cells to prevent them from dividing out of control anymore. These are just a few of the many uses for radioactive decay in the medical field, but the benefits of radioactive nuclides is not restrained to the medical field. These sources can also be used to power a nuclear power plant, but in the same breath can also be used a nuclear weapon. This wide range of uses of radioactive sources is what causes them to be so important to study and is a large reason why experiments like these are conducted.

There are three different decays that will be considered in this experiment: beta decay, positron decay, and electron capture.

1. Beta Decay

This decay is where the parent nuclide emits a beta particle (β^-), also known as an electron, to change into the daughter nuclide. In this process the parent's nuclear charge

changes by one electronic charge, meaning (Z, A) → (Z+1, A), where Z is the number of protons in the nucleus (atomic number) and A is the sum of the number of protons and neutrons (the mass number) [1]. The change in the atomic number is accomplished by a neutron in the nucleus decays into a proton, electron, and an anti-neutrino by the scheme:

$$n \rightarrow p + e^{-} + \bar{v}_e$$

Figure 1: Decay scheme of a neutron for beta decay

Where n is a neutron, p is a proton, e^- is an electron and v_e is an anti-neutrino. When the neutron decays in this way, the proton stays in the nucleus, causing the Z+1 change and therefore changing the nuclide into a different atom, the daughter nuclide. After the emission of the beta and anti-neutrino particle, the daughter nucleus may be left in an excited state $(Z+1, A)^*$, which will eventually decay to the ground state, or stable state [1]. Every nuclide wants to be in a ground state, so in order to achieve this, the excited state must give off energy to reach the ground state. This is accomplished by the nuclide by giving off a gamma-ray or by internal conversion of electrons in the shells of the atom.

Internal conversion is where the excess energy of the excited state is transferred to one of the orbiting elections, usually a K shell electron, giving it a kinetic energy that is equal to the difference between the excess nuclear energy and the binding energy of the electron. The remaining excess nuclear energy appears, as assumed in this experiment, as an x-ray when the "hole" in the K shell is filled [1]. Both gamma-ray emission and internal conversion may occur in a decay scheme, but not in the same decay.

The energies of these different states becomes important for the calculations done later in the experiment. This information applies to the other decays as well, not just beta decay. Radioactive decay is exothermic, meaning the parent nuclide must be heavier than the daughter. This difference in mass supplies the energy needed for the decay [1]. Specifically for beta emission, the decay energy is represented by:

$$E = M_n(Z, A) - M_n(Z + 1, A) - M_e$$

Equation 1: Decay energy for beta decay

Where E is the decay energy, $M_n(Z, A)$ is the nuclear mass of the parent nuclide, $M_n(Z + 1, A)$ is the nuclear mass of the daughter nuclide and M_e is the rest mass of the electron. Equation 1 will be used to calculate the total decay energy used in the decay process in order to determine the kinetic energy of the beta particle as it was emitted.

In this experiment beta decay will be referred to as scheme 1, which has two possible decay paths from the excited state of the daughter to its ground state. Gamma decay, where only gamma-rays are released, will be referred to as scheme 1a and internal conversion decay with subsequent x-ray emission will be referred to as scheme 1b [1].

2. Positron Decay

In this decay process, a positron is emitted from the parent nuclide. The positron is the antiparticle of the electron, represented by B^+, with a charge of +1 and mass M_e. In this decay, the atomic number is decreased by one, instead of increased by one like in beta decay. This is represented by (Z, A) → (Z-1, A), where Z and A are the same variables as in beta decay. The change in atomic number for positron decay is accomplished by a proton decaying into a neutron, a positron and a neutrino as shown in the scheme [1]:

$$p \rightarrow n + e^{+} + v_e$$

Figure 2: Decay scheme of a proton for positron decay

Where p is a proton, n is a neutron, e^+ is a positron and v_e is a neutrino. The proton is replaced by neutron in the nucleus, which causes the Z-1 atomic number change.

The positron, being anti-matter, does not have a long life expectancy in our world of matter. It usually goes a short distance as it

loses kinetic energy and stops in the vicinity of an electron [1]. Once the positron gets close enough to the electron, annihilation takes place. Annihilation destroys the two particles and releases energy in the form of gamma-rays as shown in Figure 3.

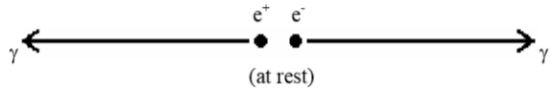

Figure 3: Annihilation of an electron and positron

There must be two gamma-rays released to conserve momentum and the sum of the two gamma-ray energies must equal the energy yielded when the positron and electron annihilate [1]. In the case where two gamma-rays are emitted the energy is calculated by the following equation:

$$E_\gamma = M_e c^2 = 0.511\ MeV$$

Equation 2: Calculation of the energy of the gamma-ray released from positron emission

Where E_γ is the energy of the gamma-ray, M_e is the mass of an electron, c is the speed of light and MeV is megaelectronvolts, which is a unit of energy. This energy of 0.511 MeV or 511 KeV is the important peak that will be observed in the gamma-ray spectrum if positron decay is occurring in the selected sample [1]. In this experiment, positron decay will be referred to as scheme 2.

3. Electron Capture:

In this final decay process, electron capture takes place. Electron capture occurs when the nucleus of the parent nuclide captures one of the electrons from the outer shells. When the nucleus captures the electron the following reaction takes place [1]:

$$p + e^- \rightarrow n + v_e$$

Figure 4: Reaction of electron capture decay

Where p is a proton, e^- is an electron, n is a neutron, and v_e is a neutrino. The electron reacts with a proton to create a neutron and a neutrino. Since a proton is replaced by a neutron in the nucleus, then the atomic number goes down by one, giving (Z, A) → (Z-1, A), just like in positron decay.

Since the electron captured usually comes for the K shell, this decay is frequently referred to as "K capture". The "hole" in the K shell is then filled by an electron from a higher shell with the emission of monoenergetic x ray. The daughter may still be left in an excited state, and in this experiment it is assumed that it decays to its ground state with the emission of a monoenergetic gamma-ray [1].

Experimental Procedure:

1. Experimental Apparatus

The detector used in this experiment was a HPGe detector, which is a more advanced detector for identifying incident gamma rays than its predecessors, the NaI(Tl) and Ge(Li) detectors. The HPGe detector consisted of a large metal Dewar flask with a horizontally aligned aluminum cylinder extending sideways from the top. The cylinder contained both the Ge detector and a preamplifier which produced output pulses proportional to the energy deposited in the detector by an incident gamma-ray through one of the three process of photoelectric effect, Compton scattering and pair production [1]. In the photoelectric process the gamma or x-ray gives all of its energy to the recoil electron. It is the recoil electron that produces the electron hole pairs in the detector that yields the output pulse [1]. In the Compton scattering process there is a distribution of pulse amplitudes up to a maximum pulse height [1]. This maximum pulse height produces the Compton edge that will be seen in the spectra. Pair production is where an electron and positron interact, producing gamma-rays. The electron will produce a pulse whose magnitude is proportional to the kinetic energy of the electron, as well as the positron producing a pulse proportional to its kinetic energy. Since these two pulses are produced simultaneously, the out pulse from the detector would be the

sum of these two pulses, a full energy peak [1]. The pulses can be altered by the gamma-rays leaving the device without hitting the detector as well, creating a single-escape or double-escape peak. None of these processes were seen in this experiment, so these peaks will not be viewed in the spectra.

Pulses originating from the detector come from the preamplifier, which were further amplified and shaped by a spectroscopy amplifier (Ortec, model 570), the final result being pulses that had a voltage amplitude proportional to the energy deposited in the detector by the gamma-ray [1]. These pulses were next processed by instrumentation called a pulse height analyzer (PHA), or for this experiment the Canberra Multiport II multichannel analyzer (MCA), which divided the full range of input pulse voltage amplitudes into a large number (8,192 in this experiment) of equal intervals (bins) or channels [1]. A single count would be added to the channel assigned to the voltage interval within which the measure value falls. Thousands of pulses were recorded over the 500 second time interval, which resulted in a histogram being created by the computer program of counts (y-axis) versus channel number (x-axis), to be created [1]. The MCA was connected to the computer by means of a USB interface, more explanation of the computer program used will be included in the calibration steps. Most of the electronic modules fit into the NIM (nuclear instrumentation module) standard, all housed in a single "NIM bin" as seen in Figure 5.

The HPGe detector was also connected to an Ortec 659 high voltage power supply using a high voltage coaxial cable. The high voltage needed for the detector was -3500 Volts. It was necessary for this voltage to be applied and removed slowly, over the course of one minute, to avoid destruction of the preamplifier. To avoid damage to the equipment the voltage was raised by increment of 250 volts every few seconds. These same steps were repeated anytime the measurements were completed to turn off the voltage.

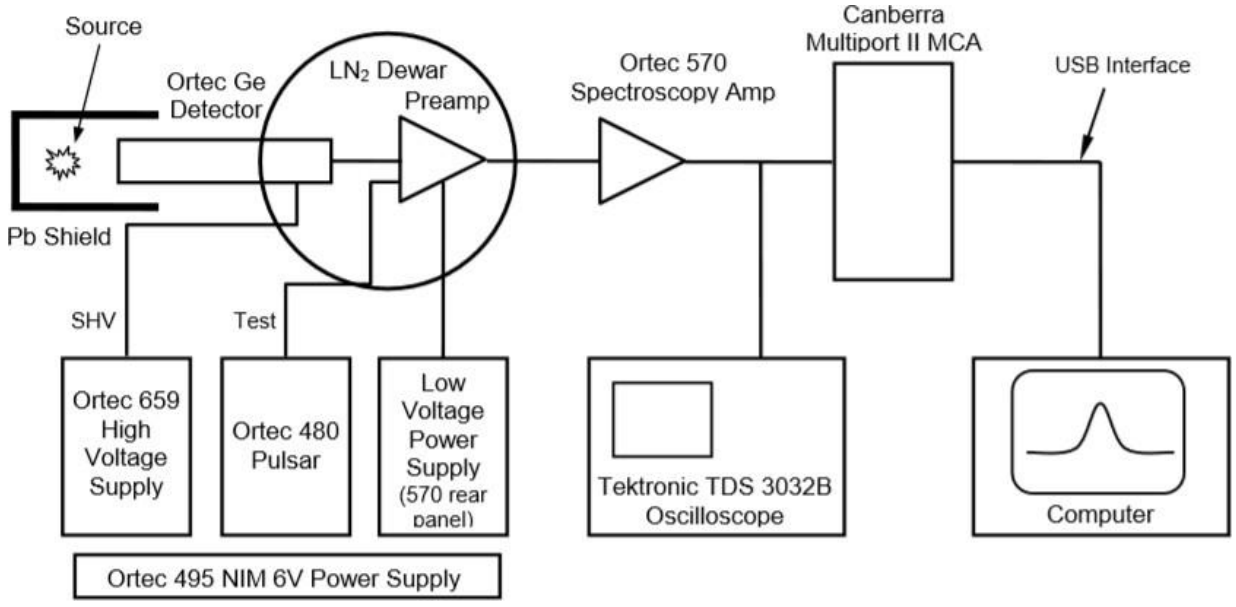

Figure 5: Experimental apparatus

2. Calibration Procedure using Co-60

Before placing the radiation source inside of the detector the equipment had to be set to specific values for each module in order to obtain a correct reading.

The pulsar was needed for calibration, so it was connected to the detector by means of

a coaxial cable. This cable ran from the Attenuated Output of the pulsar to the Test BNC connector from the detector. Once connected, the pulsar values were changed by knobs on the face of the pulsar module. The pulse height was adjusted to five volts, attenuator switch was set to x10, Off-On switch was set to on, and the Neg-Pos slider switch was set to negative in order to get a negative voltage [1].

The Ortec 570 spectroscopy amplifier was then connected to the detector by another coaxial cable from the output 1 BNC from the detector, to the input connection on the amplifier. The amplifier output was also connected to the ADC IN of MCA #1 on the Canberra MCA [1]. Once these cables were connected the amplifier values were changed on the face of the amplifier module. The gain adjust was set 1.0, coarse gain adjust was set to 100, shaping time was set to 2 μs, BLR was set to auto, input selector was set to negative and the output was set to unipolar which gives a single peak instead of a double peak [1]. The amplifier controlled the voltage read from the detector due to the radioactive sources.

Once these two modules were set to the correct values, the power could be turned on as described in the previous section, being careful to not change values too fast. After the power was on the oscilloscope could be connected. The oscilloscope was used to finely tune the voltages coming from the pulsar and the detector once the source was placed inside.

Using a “T” adapter that allowed the signal to be split between two modules, the oscilloscope was connected to the same output from the amplifier as the MCA #1. The oscilloscope was set using the “Quickmenu” button as well as using channel 1 with the input DC coupled with an input impedance set to 1MΩ. The gain was set to 2 V/cm and the sweep rate was set to 10 μs/cm using the voltage and time adjustment knobs respectively. The trigger settings were set as follows: the trig type was set to edge, mode was set to normal, source was set to channel 1, coupling was set to DC and the slope was set to positive [1].

The oscilloscope showed only the pulsar peak being read from the amplifier because the source was not inside of the detector yet. From the oscilloscope, the pulsar peak was adjusted using the pulse height adjust knob on the front of the pulsar module. The pulsar amplitude was adjusted so that the peak was around 7-8 Volts. Then the source was placed around 3 cm in front of the detector. This caused two photopeaks to be observed along with the pulsar peak on the oscilloscope. The trigger level needed to be adjusted in order to distinguish between each separate photopeak. Once each peak could be seen accurately, then the amplifier gain adjust knob was used to alter the height of the source photopeaks. The amplifier gain was adjusted so that the larger photopeak from the source had an amplitude of 6.5 Volts [1]. Since the gain adjust knob caused an increase in amplitude of all of the peaks, it was necessary to readjust the pulsar height until it fell around 0.5 Volts above the upper source peak.

All of these adjustments were necessary because it allowed the required gamma-ray peaks read into the computer to be in the correct positions. This adjustment section caused the first readings to be off in the experiment and only two peaks could be seen. This was fixed by readjusting the gain control knob to have a course gain of 50 instead of 100 and altering the gain until the peaks were spaced as they should have been.

Once the oscilloscope readings were correct, data acquisition could begin. The computer used in the lab had a program called “Gamma Acquisition & Analysis” which would take in the data from the detector and reproduce a histogram of counts versus energies of the gamma-rays. To begin the calibration the datasource GAMMA_GE was selected to obtain a new set of data. Once open, the radioactive source in the detector and the all of the settings correct the program could be started. The program ran for 500 seconds, as preset before the experiment. At the completion of the 500 seconds, three peaks were observed. The peak on the furthest right

was the pulsar and the other two peaks were from the radioactive source's gamma-rays.

These peaks were not showing up on the correct energy levels. This is because the calibration step was not completed as of yet. To complete the calibration, the peaks must be moved to the known energy values of the gamma-rays from Cobalt-60. These values were 117 and 133 KeV for Cobalt-60. The auto calibration would not work because of an equipment malfunction that was later fixed after this experiment was completed. However, by entering it manually allowed for data to still be taken without much alteration. The manual calibration was done by entering the known energy value and channel value read off of the photopeaks. The cursor was placed at the top peak of the photopeak and the program showed the value of the channel number that belonged to that peak. This was the value that was entered as the channel number when calibrating. Once both known energy and channel values were entered, the histogram was automatically changed to display each photopeak in the correct 117 and 133 KeV value. This completed the calibration of the equipment and it was important to not alter any of the NIM bin instrument settings after this point or it would have required a recalibration.

Now that the calibration was complete the peak energies and FWHMs (full width half maximums) could be established for each photopeak. Each peak was bracketed with a ROI (Range of Interest), causing the peak to turn red. The computer program would then read out the values required. Each of the peaks gave a peak energy, FWHM and area value that were noted. Other features that were noted were Compton edges, which are values of energy due to Compton scattering of gamma rays. These values were established by placing the computers cursor on the top peak of the Compton edge just before the energy value dropped.

These recorded values can be seen in the annotated spectra, Figures 6 and 7, for Cobalt-60.

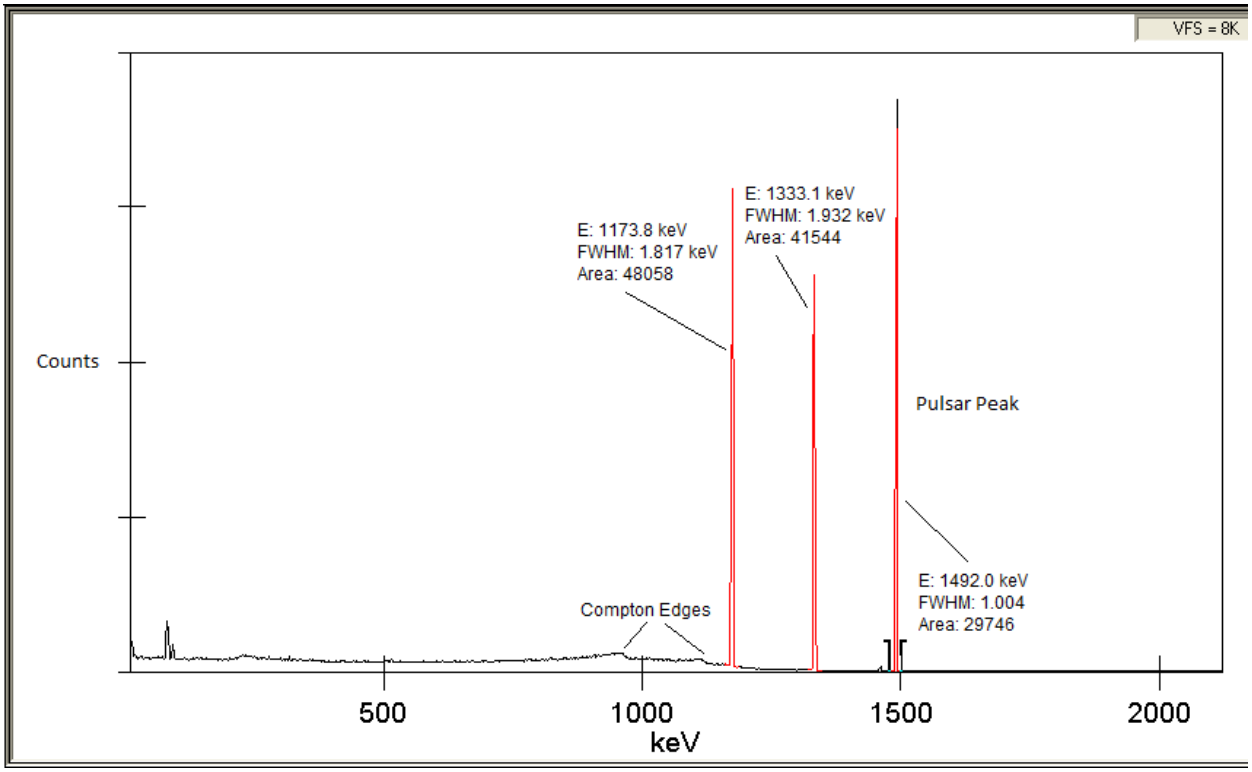

Figure 6: Annotated spectra for ^{60}Co used for calibration

Figure 6 shows the full recorded spectra after calibration of Cobalt-60. Each peak is labeled with its peak energy (E), FWHM value and area of the peak. The peak on the furthest right is the peak from the pulsar. In Figure 6 the data is shown in a linear format, making it hard to see the Compton edges. To better see the Compton edges, the computer program allowed the data to be seen in a log format as seen in Figure 7.

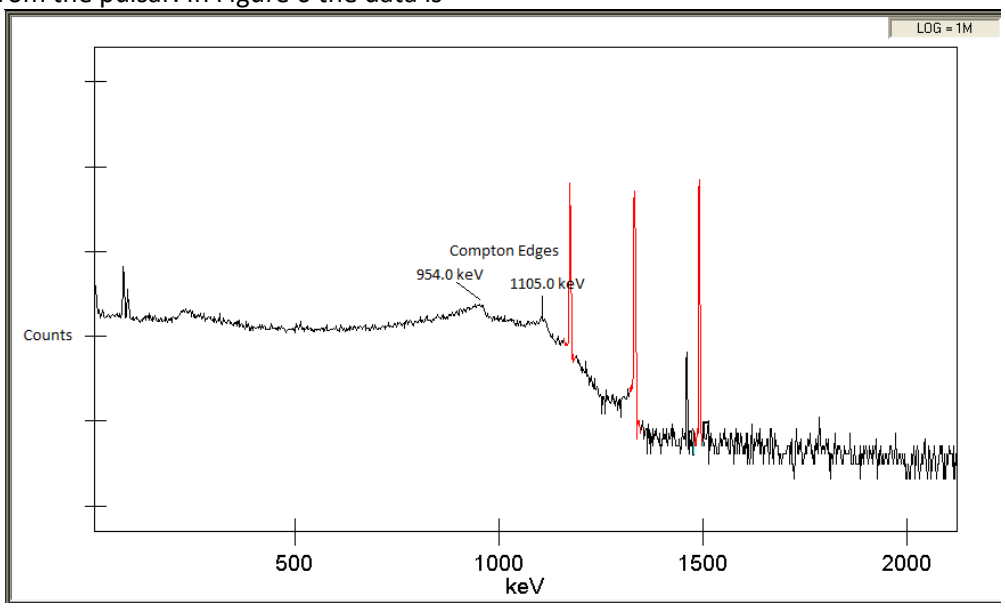

Figure 7: Log format for ^{60}Co to identify the Compton edges

The log version of the data shown in Figure 7 clearly showed the Compton edges due to the Compton scattering of the gamma rays. These Compton edges happed at an energy value of 954.0 keV and 1105.0 keV.

The computer program also was able to include a calibration curve:

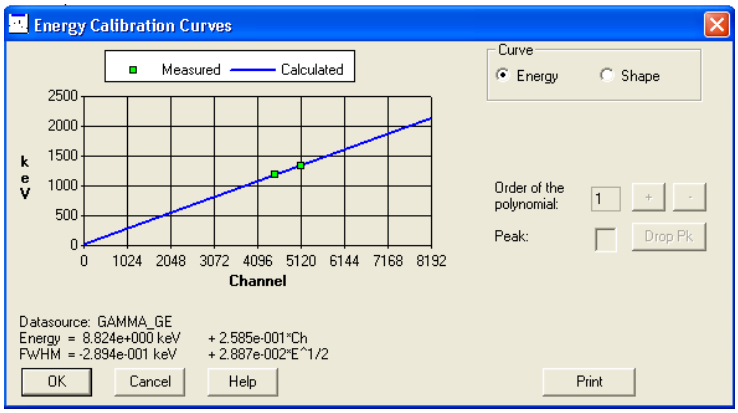

Figure 8: Energy calibration curve for ^{60}Co

This revealed that the calibration is linear, meaning that each channel gains energy based on the slopes value. It also revealed that the y-intercept is not zero, but rather 8.824 keV. This meant that at channel zero it would have still read a value of 8.825 keV. This effected the ability to see lower value energies, like when looking for x-rays later in the experiment.

3. Energy Resolution

The resolution of the detector can be calculated using the values obtained during the calibration of the equipment. The most important value that pertains to resolution, is the FWHM value from the data.

$$R_{det} = \sqrt{R^2_{det+elect} - R^2_{elec}}$$

Equation 3: Calculation for the resolution of the detector

Equation 3 shows how the resolution of the detector could be calculated by knowing $R_{det+elec}$, which is the FWHM value of the photopeak caused by the radioactive source and R_{elec}, which is the FWHM value of the pulsar peak [1]. The FWHM measured for the pulsar peak indicates the limit on energy resolution imposed by the electronics alone, since it is just part of the electronic structure and not connected into the detector. The FWHM measured for a typical photopeak from the source measures the limit on energy resolution imposed by both the detector and the electronics, because the measurement comes from both the electronic structure and from the detector itself [1]. So if the two resolutions are subtracted then the only thing left will be the resolution of the detector alone with the resolution of the electronics subtracted out. Using the relation from Equation 3 does exactly this.

The data from the calibration of Cobalt-60 was used to calculate this value. There are two peaks relating to $R_{det+elec}$, so two calculations were made and those values were compared to see how well they agreed. Using $R_{det+elec}$ as 1.817 keV for the first photopeak from the radioactive source seen in Figure 6 and R_{elec} as 1.004 keV, the resolution of the detector was found to be 1.5144 keV. For the second calculation, $R_{det+elec}$ was 1.932 keV and R_{elec} was the same value of 1.004 keV. This second calculation of the detector resolution using the second photopeak resulted in a value of 1.6506 keV. These two values do not agree exactly because the FWHM values of each peak would have to be identical in order to have the same value of detector resolution.

Analysis and Results:

1. Peak energy and Uncertainty

Once the calibration was complete the gamma-ray spectra were measured for four other radioactive sources: ^{57}Co, ^{137}Cs, ^{54}Mn, and ^{22}Na. Each spectra was labeled with the peak energy, FWHM, area, counts, and Compton edges. The peak energies for each photopeak was calculated by the computer program used to obtain the spectra. This value came from the information displayed when the top of each peak was marked by the cursor. The centroid value gave the exact peak energy reading that occurred without the need of any calculation of the value. However, the value could have been calculated using the analyze feature of the computer program. This would have given a list of channel energy values with the counts in each, which then could have been used to calculate the average value of the energies using equation:

$$\bar{x} = \frac{1}{N}\sum_{i=1}^{N} x_i$$

Equation 4: Calculation of the mean value of data [2]

Where $\bar{x}$ is the mean value of the data, N is the total number of counts, and x_i is each energy value within the data. The N value is the total number of counts in the entire photopeak, not just in one channel. This means that each channel count that made up the entire peak was added up to give the total N value for that photopeak. The mean value of the data would have been used as the peak energy of each individual peak in each of the different spectra. This value would closely resemble to energy peak value shown by the computers estimation, the centroid value. This is why the computers estimation was used instead of calculating each individual peaks value to save on time.

Each peak energy value comes with an uncertainty, which is true for any measurement

made with a detector. Since these peaks represented a Gaussian distribution and the counts were much higher then 100, the uncertainty can be calculated using the FWHM value for each peak [2]. Therefore, if N is large (N>100), σ or the standard deviation can be estimate by the equation:

$$\sigma = 0.4248\ x\ FWHM$$

Equation 5: Standard deviation if N>100 and a FWHM value for each peak was known [2]

Where σ is the standard deviation and FWHM is the full width half maximum value of each photopeak. This equation was used as an estimation, which will be slightly off from the real calculation due to some of the photopeaks that were not an exact Gaussian distribution. This equation was accurate enough to not cause any significant difference, so the value was acceptable. Once the standard deviation was known for each photopeak, the uncertainty of the peak energy could be calculated.

$$\sigma_m = \frac{\sigma}{\sqrt{N}}$$

Equation 6: Uncertainty calculation for each photopeak [2]

Where σ_m is the uncertainty, σ is the standard deviation relating to each photopeak, and N is the total counts for each photopeak. Equation 6 gave each uncertainty in the peak energies of each significant photopeak, in each spectrum.

2. Cesium-137

Cesium-137 was the parent nuclide that decays into Barium-137, which was the daughter nuclide. This decay was represented by:

$$^{137}_{55}Cs \rightarrow {}^{137}_{56}Ba$$

Figure 9: Decay of Cesium-137 into Barium-137 [1]

Where the bottom numbers represent the atomic number (Z) and the top number represents the atomic mass (A). As seen from Figure 9, this decay is similar to a (Z, A) → (Z+1, A), or a beta decay process. This forced this decay to follow a scheme 1a and/or 1b decay process, following a beta particle emission as discussed in the introduction.

To establish which scheme this decay process followed, it was necessary to look at the gamma-ray spectra obtained during the experiment.

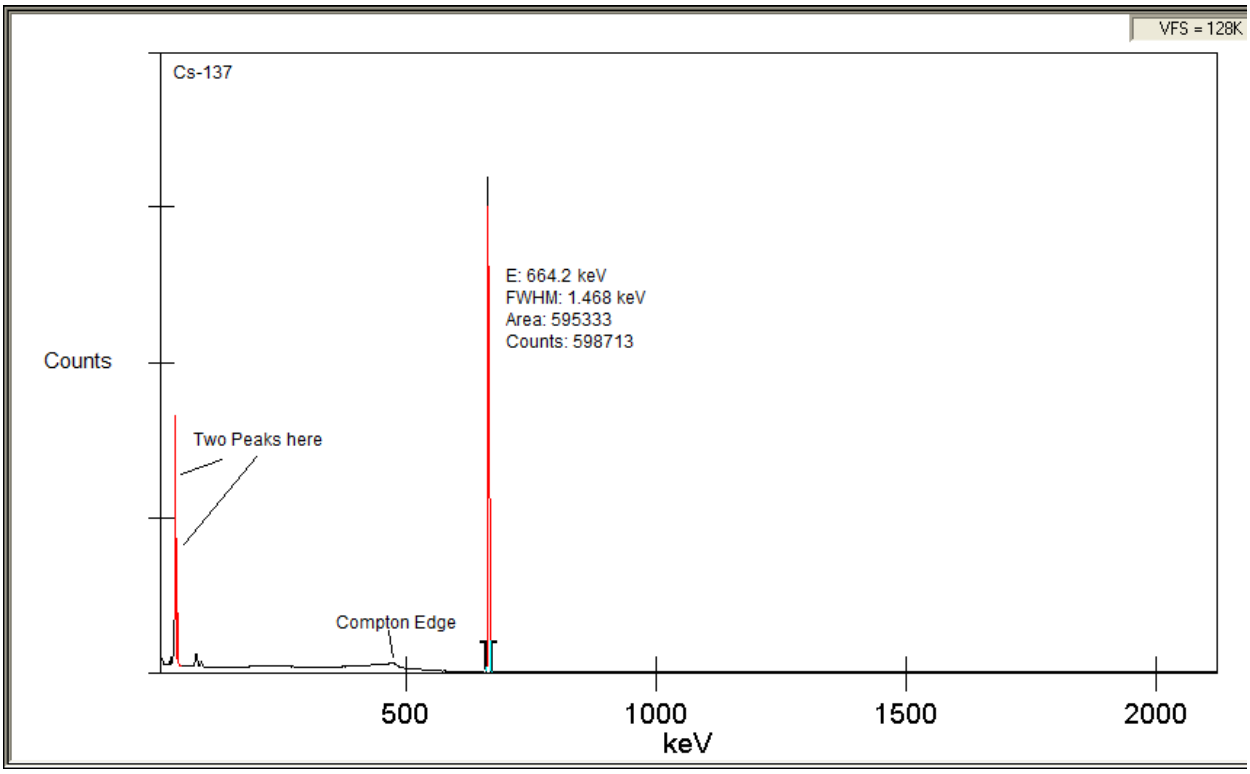

Figure 10: Linear gamma-ray spectra for ^{137}Cs with three photopeaks

This linear spectra revealed 3 peaks with the main peak being the largest energy value. To see the two lower energy peaks and the Compton edge more efficiently, the log format of the graph and the expand button was used on the computer program.

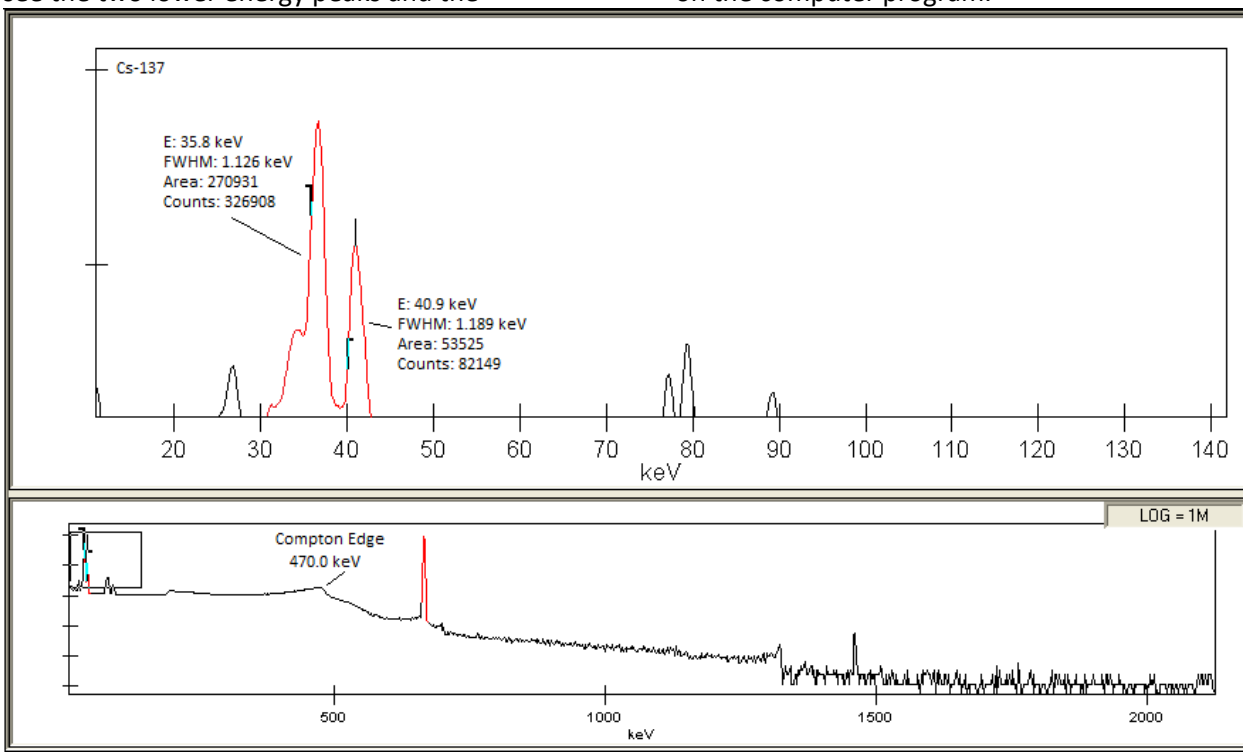

Figure 11: Log gamma-ray spectra magnified for ^{137}Cs showing other two peaks and Compton edge.

The log version of the spectra revealed the two lower energy peaks and Compton edge in much more detail. The peak energies (E) and FWHM values were established in these figures, which allowed for the calculation of uncertainty using equations 5 and 6. These values were combined with the peak energy values for each peak in a table.

Photopeak	Peak Energy
1	35.8000 ± 0.0008 keV
2	40.900 ± 0.001 keV
3	664.2000 ± 0.0008 keV

Table 1: Peak energies and uncertainties for each photopeak of ^{137}Cs

Table 1 shows the peak energy and uncertainty for each photopeak seen in the spectra obtained during the experiment. This information came from Figures 10 and 11 going from the least energetic peak on the left to the most energetic peak on the right.

The Compton edge value for Cs-137 was seen in Figure 11 to be a value of 470.0 keV. This value could be theoretically predicted using the energy value of the peak energy that it came from. In this decay, the Compton edge was coming from the 664.2 keV value of the largest photopeak. The two, less energetic peaks, did not have Compton edges that were identifiable in the spectra obtained for this experiment. From the Compton scattering equation, the formula for the energy of the final photon that was scattered could be established.

$$E' = \frac{E}{1 + \frac{E(1-\cos\theta)}{m_e c^2}}$$

Equation 7: Energy of the final photon after scattering [3]

Where E' is the energy of the final scattered photon, E is the energy of the incident photon which is based on the photopeaks in this experiment, $m_e c^2$ is the rest mass of an electron, and θ is the angle of scatter with respect to the incident photon. To theoretically estimate the Compton edge, θ was set equal to 180° as if the gamma ray had reflected complete back towards the incident photon. The value of $m_e c^2$ was just the rest mass of an electron, which was the value of 511 keV and E was the peak energy value of the photopeak that relates to the Compton edge measured in the spectra.

Using Equation 7 and the information stated above, the value of E' was calculated to be 184.52 keV for the photopeak at 664.2 keV. Now that the energy of the final photon was known, the Compton edge value could be established by subtracting this final photon's energy (E') from the peak energy value of the photopeak (E). This gives the energy difference in the two photon's (gamma-rays) that created the measured peak values in the spectra.

$$C = E - E'$$

Equation 8: Energy of the Compton edge

Here C is the theoretical energy of the Compton edge seen in the gamma-ray spectra, E is the peak energy value of the photopeak seen in the spectra and E' is the calculated energy of the final photon from Equation 7. Using Equation 8 and the result of Equation 7, the theoretical Compton edge energy was calculated to be at 479.68 keV. As seen in Figure 11, the measured Compton edge was 470.0 keV so the theoretical value is a good estimate for the measured value.

After analyzing the spectra, there were small energy values around 10 keV that had counts above 2000. These counts represented what would be established to be x-rays. So this decay process was producing x-rays. These values below 10 keV were very difficult to establish because the spectra graph cut off around 15 keV on the actual graph but the computer's cursor could be dragged past that value to read off count values that were lower. From the information from Figure 9, which

showed that this decay was a Z+1 decay, and x-rays were being produce, it was established that this decay could have been a scheme 1b. However, this decay also had gamma-rays that were being produce so it could also decay by scheme 1a. This made it apparent that for Cs-137, the nuclide could have decayed by scheme 1a, as well as scheme 1b. Either scheme would work for this decay, so both nuclear energy level diagrams were produced.

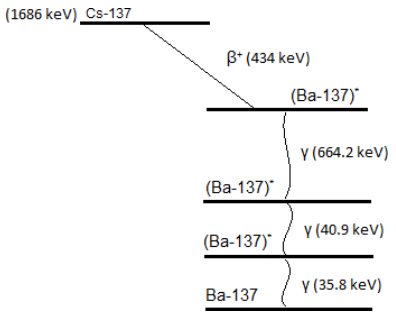

Figure 12: Scheme 1a nuclear energy level diagram for Cs-137

For scheme 1a the beta particle was released and to get from the excited daughter state to the ground state the three gamma-rays were emitted, which relate to the gamma-rays measured in the spectra.

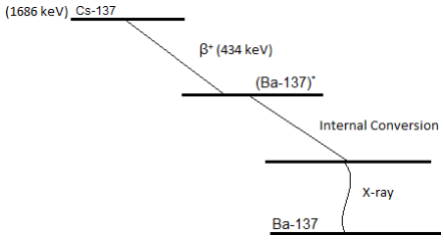

Figure 13: Scheme 1b nuclear energy level diagram for Cs-137

In scheme 1b, the beta particle is emitted for the parent nuclide and to get from the excited daughter to the ground state the nuclide did an internal conversion of electrons, then released an x-ray.

The values calculated in Figures 12 and 13 come from the kinetic energy of the beta particle and the total decay energy between the parent and daughter nuclide. This was calculated using Equation 1 for the total decay energy of the reaction. The nuclear mass values of both Cesium and Barium were 136.9070895 amu and 136.9058274 amu respectively. Taking the difference of these two values gave the difference in mass (Δm) that would be used to find the energy of the decay. This value was 1.2621×10^{-3} amu. This value was then converted to an energy value using the equation:

$$E_d = \Delta m(931.5 \frac{MeV}{c^2 amu})$$

Equation 9: Converting from change in mass (amu) into energy (MeV)

Where E_d is the energy of decay and Δm is the change in mass between the parent and daughter nuclide in amu. Using Equation 9, the energy value was calculated to be 1175.65 keV. Going back to Equation 1, that was the difference in energy between the two nuclide, as well as the rest mass of an electron subtracted off. So, in order to know just the difference in energy between the two nuclide the rest mass of an electron must be added to this value. This gave a value of 1686 keV, which is the value used for Cs-137 in Figures 12 and 13.

To find the kinetic energy of the beta particle the known energies of the gamma-rays were used. The value of the energy of decay, E_d, had the energetic values of the three peaks subtracted from it. This left a value of only the kinetic energy of the beta particle left over. As stated before E_d already had the rest mass of a beta particle subtracted from it, so there was no need to subtract it once more. Once the three gamma-ray's energies were subtracted, this left the value of 434 keV of kinetic energy left over. This is the value found in Figures 12 and 13. The values next to the gamma-rays are just the peak energy values read from the spectra, or Table 1.

3. Na-22

Sodium-22 was the parent nuclide that decays into Neon-22, which was the daughter nuclide. This decay was represented by:

$$^{22}_{11}Na \rightarrow {}^{22}_{10}Ne$$

Figure 14: Decay of Na-22 into Neon-22

As seen from Figure 14, this decay process was a (Z, A) → (Z-1, A). This made it possible for two different schemes, either scheme 2 or scheme *3.* In order to determine which decay scheme Ne-22 used, the gamma-ray spectra was observed.

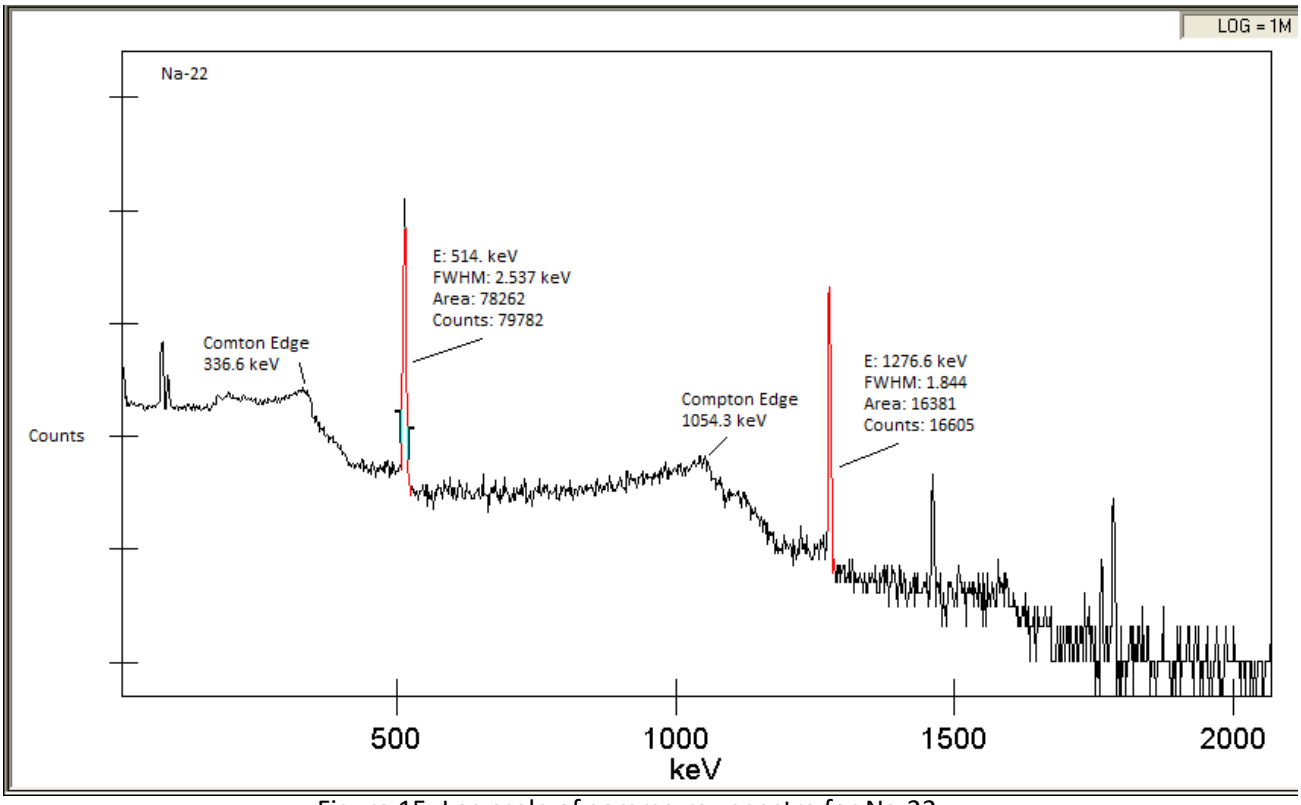

Figure 15: Log scale of gamma-ray spectra for Na-22

Just as before, using the values found in Figure 15 the FWHM values and peak energy values were used to calculate uncertainties for each photopeak. There were only two photopeaks for Na-22.

Photopeak	Peak Energy
1	514.000 ± 0.004 keV
2	1276.600 ± 0.006 keV

Table 2: Peak energy and uncertainty for photopeaks from Na-22

Table 2 shows the peak energy and calculated uncertainty for each photopeak from Figure 15.

The Compton edge values for Na-22 were 336.6 keV for the photopeak at 514 keV and 1054.3 keV for the photopeak at 1276.6 keV. Equations 7 and 8 were used to obtain the theoretical values for each of the Compton edges just like for the Cs-137 nuclide. This resulted in a theoretical value of 343.33 keV for the lower energy peak and 1063.71 keV for the higher energy peak. These theoretical values come very close to the measured values, so the theoretical value is an acceptable estimate for the measured value.

Since this decay was a Z-1 decay, it was open to be a scheme 2 or scheme 3 decay. After looking at the spectra, the easily identified 511 keV was present for Na-22. This narrowed the decay to be positron decay, or scheme 2. In scheme 2, a positron is released from the parent nuclide and the excited daughter nuclide

releases a gamma-ray to get to the ground state.

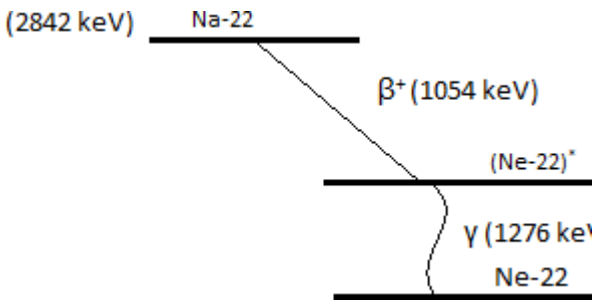

Figure 16: Nuclear level diagram for Na-22, scheme 2

Figure 16 shows the nuclear level diagram of the decay of Na-22 to Ne-22 by means of positron emission. The calculated energy values come from the total decay energy between the two nuclides. Using Equation 9, and the mass difference of 0.003051286 amu between Na-22 and Ne-22 nuclear masses, the total decay energy was calculated to be 2842.27 keV. The Na-22 energy value is just the total decay energy because it was a Z-1 instead of a Z+1 like before, which is 2842 keV as seen in Figure 16.

To find the positron's kinetic energy, the total decay energy had the energy of the larger energy gamma-ray subtracted off, as well as the rest mass of a positron subtracted off. This gave a kinetic energy value of 1054 keV left over for the positron to travel with. The second gamma-ray energy of 514 keV was not subtracted off, because this was not from the actual decay of the two nuclide. This 514 keV came from the positron annihilating with an electron, which would not count towards the decay energy.

4. Mn-54

Manganese-54 was the parent nuclide that decays into Chromium-22, which was the daughter nuclide. This decay was represented by:

$$^{54}_{25}Mn \rightarrow ^{54}_{24}Cr$$

Figure 17: Decay of Mn-54 into Cr-54

As seen from Figure 17, this decay process was a (Z, A) → (Z-1, A). This made it possible for two different schemes, either scheme 2 or scheme 3. In order to determine which decay scheme Mn-54 used, the gamma-ray spectra was observed.

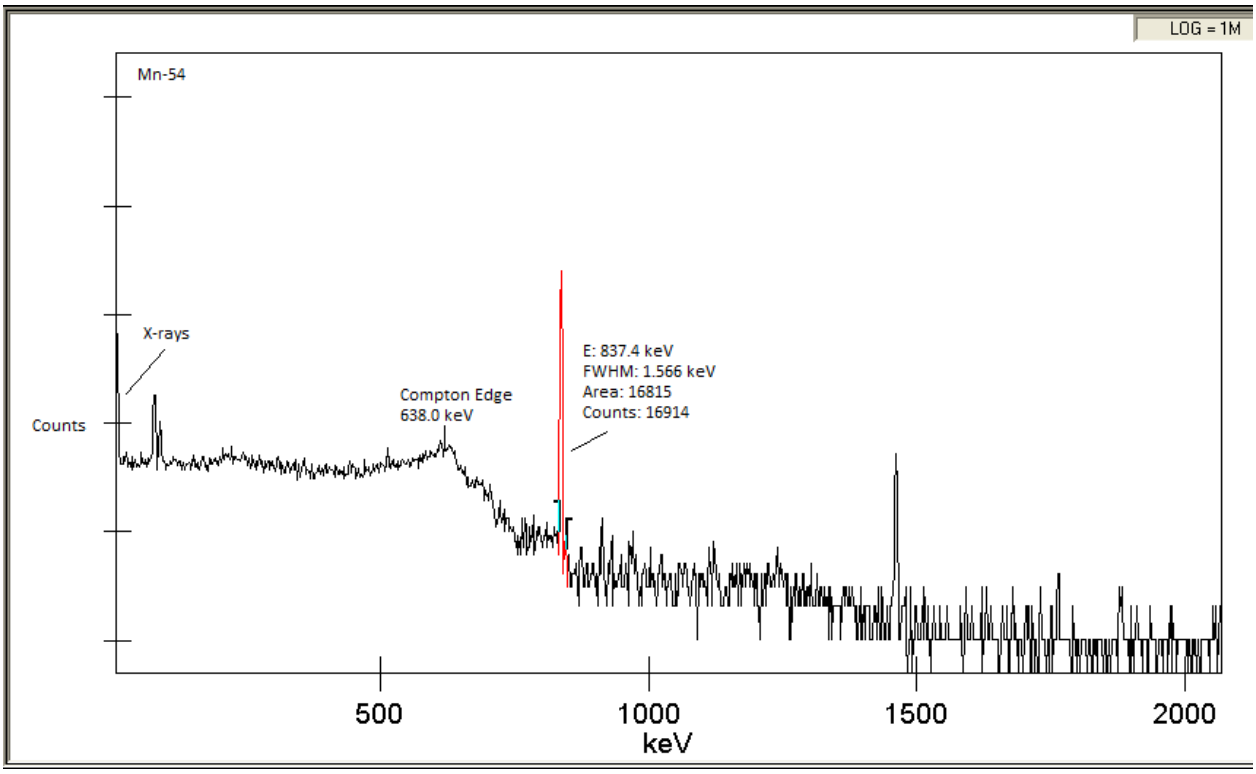

Figure 18: Log scale of gamma-ray spectra for Mn-54

Just as before, using the values of Figure 18 the FWHM values and peak energy values were used to calculate uncertainties for each photopeak. There was only one photopeak observed in Mn-54.

Photopeak	Peak Energy
1	837.400 ± 0.005 keV

Table 3: Peak energy and uncertainty for Mn-54

Table 3 shows the peak energy and uncertainty for the only gamma-ray photopeak seen in Mn-54's spectra.

There was only one Compton edge value of 638.0 keV for the photopeak at 837.4 keV. Using Equations 7 and 8 again, the theoretical value of the Compton edge was calculated. Once calculated the value of 641.6 keV was obtained. This theoretical value that was calculated is again, close to the measured value so it can be assumed that it is an acceptable estimate for the measured value.

Since Mn-54 decayed as a Z-1, this left it open to schemes 2 and 3. Since there was no visible 511 keV gamma-ray value and x-rays seemed to be present, it was safe to assume that this decay was a scheme 3 process. This meant that the nuclide decayed by means of electron capture.

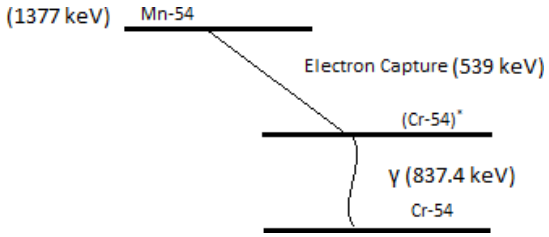

Figure 19: Nuclear level diagram for Mn-54, scheme 3

Figure 19 shows the decay scheme for Mn-54 to Cr-54 by means of electron capture. In this decay, there were no particles ejected from the decay, only gamma and x-rays. This made it unnecessary to calculate a kinetic energy, so only the total decay energy was needed to calculate everything. The x-ray energies were included into the electron capture stage of the nuclear level diagram. The mass difference

between Mn-54 and Cr-54 was 0.0014785 amu. This value was plugged into Equation 9 and revealed a value of 1377.22 keV in total decay energy. That was the total energy between the two nuclides, as seen in Figure 20. By subtracting the gamma-ray energy value obtained from the spectra, the energy used in the electron capture and release of an x-ray could be calculated. This was the value of 539 keV, as seen in Figure 20.

5. Co- 57

Co-57 was the parent nuclide that decays into Fe-57, which was the daughter nuclide. This decay was represented by:

$$^{57}_{27}Co \rightarrow {}^{57}_{26}Fe$$

Figure 20: Decay of Co-57 into Fe-57

As seen from Figure 20, this decay process was a (Z, A) → (Z-1, A). This made it possible for two different schemes, either scheme 2 or scheme 3. In order to determine which decay scheme Co-57 used, the gamma-ray spectra was observed.

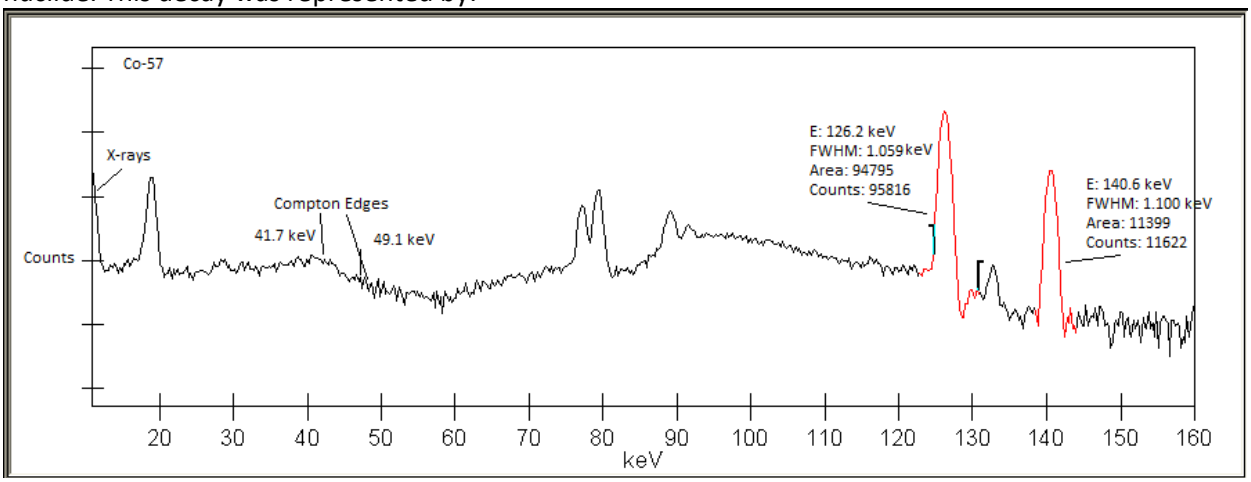

Figure 21: Log scale of gamma-ray spectra of Co-57

Using the values from Figure 21, the FWHM values and peak energy values were used to calculate uncertainties for each photopeak. There were two photopeaks observed in Co-57.

Photopeak	Peak Energy
1	126.200 ± 0.001 keV
2	140.600 ± 0.004 keV

Table 4: Peak energies and uncertainties for photopeaks of Co-57

Table 4 shows the peak energies, as well as the uncertainties for each peak in the Co-56 gamma-ray spectra.

There were two Compton edge values of 41.7 and 49.1 keV for the spectra of Co-57, but only one was clear. Calculating the theoretical value of these Compton edges gave the values of 41.7 keV and 49.9 keV. Since the 49 keV value of the Compton edge was hard to establish where it exactly was in the spectra, it could have been ignored. There was however, a slight dip in the spectra right around this value, so it was left in. The theoretical values are much more accurate for this spectra because of the smaller energy values used. This made the estimates exactly right for the measurement for one of the Compton edges and slightly off for the other.

Since Co-57 decayed as a Z-1, and there were no signs of 511 keV gamma-ray, this left only one choice for its decay scheme. Co-57 decayed by scheme 3, electron capture, just like Mn-54.

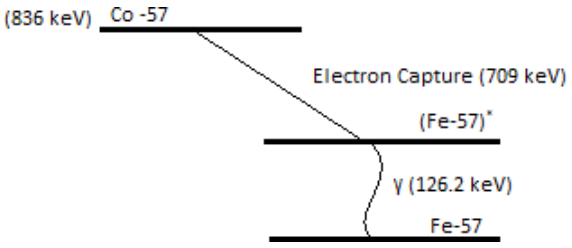

Figure 22: Nuclear level diagram for decay of Co-57, scheme 3

Figure 22 shows the decay scheme 3 for Co-57. As stated in the introduction for electron capture, the excited daughter nuclide can only decay to its ground state with the emission of monoenergetic gamma-ray. This meant that only one of the photopeaks could be chosen to act as the gamma-ray that brought the excited state to the ground state. Since the peak with energy 126.2 keV had much more counts than the other photopeak, the energy of 126.2 keV was chosen as the monoenergetic gamma-ray. To calculate the energies the change in mass between the parent and daughter nuclide of 0.0008974 amu was used. This change in mass value, along with Equation 9, gave a total decay energy of 835.92 keV which can be seen in Figure 22 for Co-57. Subtracting off the monoenergetic gamma-ray of 126.2 keV gave the total energy used in the electron capture step, 709 keV.

6. Co-60

Even though Co-60 was used as a calibration step, the same calculations can be made for its decay.

$$^{60}_{27}Co \rightarrow ^{60}_{28}Ni$$

Figure 23: Decay of Co-60 into Ni-60

This decay was similar to the Cs-137 decay in that it was a Z+1 decay, meaning it was a beta emission by either scheme 1a and/or 1b. Looking at the spectra's from Figure 6 and 7, there were no x-ray released in this decay. This meant that for Co-60, it had to decay by scheme 1a only. There were three peaks for Co-60, each with their own uncertainty value.

Photopeak	Peak Energy
1	1173.800 ± 0.003 keV
2	1333.100 ± 0.004 keV
3	1492.000 ± 0.002 keV

Table 5: Peak energy and uncertainties for Co-60

There were two Compton edges for Co-60 at 954.0 and 1105.0 keV. Calculating the theoretical values gave 963.9 and 1118.7 keV respectively. Since these were higher energy values, it caused the theoretical to be off more than they would be if it were small energy values. These values were still close enough to say that the theoretical values are good estimates of the measure values.

Since it was established that Co-60 decays by scheme 1a, that means that it released a beta particle, then decayed from the excited daughter states by gamma-ray emission.

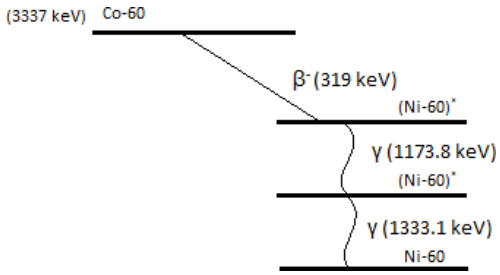

Figure 24: Nuclear level diagram for decay of Co-60, scheme 1a

The values established in Figure 24 comes from the calculation of the total decay energy of the two nuclides. The difference in mass was 0.003034 amu and using Equation 9 gave a value of 2826.46 keV for total decay energy. To get the energy for just the difference in mass of the two nuclides, the rest mass of an electron was added, because of the Z+1 property, to the total decay energy, giving 3337 keV as seen in Figure 24. The kinetic energy of the beta

particle was calculated by subtracting off the two gamma-ray energies from the total decay energy, leaving a value of 319 keV for the beta particle's kinetic energy.

Conclusion:

This experiment was able to use a detector to obtain a gamma-ray spectra in order to determine decay schemes for each of the five radioactive isobars. Given the results of the gamma-ray spectra for Cobalt-60 and the knowledge that it followed a Z+1 nuclear charge change, this experiment was able to establish that Co-60 decays to Ni-60 by means of beta decay and subsequent release of gamma-rays (Scheme 1a). The specific nuclear level diagram and calculated energies released during the decay is shown in Figure 24.

After viewing the results of the gamma-ray spectra for Cs-137 and the knowledge that Cs-137 decays to Ba-137 by a nuclear charge change of Z+1, this experiment was able to prove that Cs-137 can decay to Ba-137 by two different decay schemes. Since x-rays were viewed in the spectra it could be established that Cs-137 could follow decay scheme 1b, beta decay with subsequent internal conversion with x-ray emission. However, Cs-137 also had gamma-ray emission energy values, meaning it could also decay by means of scheme 1a, beta emission with gamma-ray emission to bring the daughter nuclide from an excited state to its ground state. The nuclear level diagrams of these two different decays can be seen in Figures 12 and 13.

The gamma-ray spectra for Na-22 showed an important gamma-ray value of 514 keV. This established that Na-22 must decay to Ne-22 by means of positron emission (Scheme 2). When the positron stops next to an electron it annihilates, causing a gamma-ray of 511 keV to be released. This was the gamma-ray seen in the spectra, leading to the conclusion that Na-22 must decay by positron emission. Once the positron was emitted it decayed from its excited daughter state to its ground state by means of gamma-ray emission. This gamma-ray was not the 514 keV one as discussed earlier. The 514 keV gamma ray was not part of the decay energy process, so it was important to not include it in the calculations of the different energies. The nuclear level diagram of the decay scheme can be seen in Figure 16.

For the decay of Mn-54 into Cr-54, the gamma-ray spectra revealed some x-rays being produced. Since the nuclear charge change for this decay was a Z-1 and there was no indication of a gamma-ray at the 511 keV energy, this meant that Mn-54 must decay to Cr-54 by means of electron capture (Scheme 3). This same decay process followed for Co-57 to Fe-57 because of the same reasons as mentioned above. This meant that both Mn-54 and Co-57 decay to their daughter nuclides by means of electron capture. Their nuclear level diagrams can be seen in Figures 19 and 22 respectively.

Overall, this lab went over successfully, with not many issues. One of the problems that came from the experiment was the inability to use the auto energy calibration by use of the Co-60 certificate file. The experiment was able to continue because there was a way to bypass the auto calibration and to do it manually. This may have caused the data to be off compared to the auto calibration style, so being able to use the auto calibration should be used for accuracy. To make improvements on this experiment the laboratory worksheet should have specific directions on how to manually enter the calibration steps, incase this happens to a future experimenter.

Future experiments could be done using different analysis other than gamma-ray spectra in order to determine other decay schemes. It was stated that in beta decay the parent nuclide can decay directly to the daughter nuclide by means of beta emission alone, but this could not be determined from a gamma-ray energy spectrum alone [1]. Also, during internal conversion extra energy during beta decay could be converted to kinetic energy of Auger electrons [1]. This again could not be established by just gamma-ray spectra. This means a large gap of decay schemes were left out because not enough information was

obtained during this experiment. Replicating this experiment with other analysis programs would help in distinguishing these other decay schemes.

Acknowledgements:

I would like to thank Dr. Beyermann for his help on this lab. He personally went through some of the calculations to help diagnose some of the issues we were having. I would also like to thank my partner Daniel Lee, who helped with many parts of the experiment.

References:

[1] W.P. Beyermann, "Gamma-Ray Emission from Radioactive Isobars", (2006)

[2] W.P. Beyermann, "Statistical Treatment for Experimental Data", (2003)

[3] UC Berkeley, AstroBaki, https://casper.berkeley.edu/astrobaki/index.php/Compton_Scattering (2014)

[4] World Nuclear Association, http://www.world-nuclear.org/info/Non-Power-Nuclear-Applications/Radioisotopes/Radioisotopes-in-Medicine/, (2015)